

## 9 Extensions of the Cylindrical Model

by Lutz Jaitner, August, 2018 through April, 2019

The cylindrical model, as defined by simplifications (3) through (21), was build to be simple, rather than precise. Accordingly, some terms are missing in the Hamiltonian.

The following extensions of the cylindrical model are attempting to explore some of these missing terms, which had been “approximated away” in the first instance. The extensions themselves are also approximations.

### 9.1 Helical Structure, Spin-Orbit Interaction, Inductance

According to simplification (14) the electron spins (and their related magnetic moment) are neglected. According to simplification (15) also the magnetic field of the azimuthal electron orbits is neglected. Both simplifications make sense in the perfectly straight geometry of CPs prescribed by the cylindrical model of CPs.

In reality however, CPs often have a helical shape, as is depicted by Figure 2. This is like a solenoid with two layers of windings. In these cases the axial movement of the electrons is tied to their azimuthal movement. The magnetic field then has an axial component, which will couple with the electron spins. The details of the coupling are complicated and not yet fully understood.

Here, a rough estimate shall be derived about the maximum energy release per electron, which can be expected when the electron spins are aligning with the axial component of the magnetic field.

The strength of the magnetic field within a long solenoid in vacuum is given by:

$$(185) \quad B = \mu_0 \frac{N}{l} I, \text{ where } \frac{N}{l} \text{ is the number of winding turns per unit of length, } I \text{ is the current flowing through the windings and } \mu_0 \text{ is the vacuum permeability}$$

Assuming that the current reaches 10 kA and there are 100 winding per millimeter, the resulting strength of the magnetic field is in the order of 1 kT. The electrons are only partially immersed in this field, so that the expectation value of the magnetic field  $\langle B \rangle$  is maybe only one tenth of this value (i.e. 100 T).

The potential energy of an electron is lowered by the following amount, when the electron spin aligns itself to the effective magnetic field:

$$(186) \quad \Delta E = \mu_B \langle B \rangle \approx 0.006 eV$$

The inductance per unit of length of a solenoid in vacuum is:

$$(187) \quad \frac{L}{l} = \mu_0 \left( \frac{N}{l} \right)^2 A, \text{ where } A \text{ is the cross section area of the solenoid}$$

Assuming, that a CP has a solenoid radius of 10 micrometer and 100 turns per millimeter, the inductance per unit of length would be about 4 nH per millimeter of solenoid length, i.e. about 0.6 nH per millimeter of plasma length.

In comparison, the inductance of a straight CP in the most stable configuration (see chapter 10.1) is about 4nH per millimeter of plasma length. This means, the inductance of a CP will be dominated by equation (54) rather than by equation (187).

Equation (187) will become inaccurate, if the spacing between the windings is becoming much larger than the diameter of the solenoid “wire”, as is often the case with CPs.

The cyclotron frequency of the electrons is given by:

$$(188) \quad f_c = \frac{e \langle B \rangle}{2\pi m_e}$$

At  $\langle B \rangle = 100T$  the cyclotron frequency of the electrons is about 2.8 THz.

The radius of the cyclotron orbits is:

$$(189) \quad r_c = \frac{m_e v}{e \langle B \rangle} \approx 6.8 \mu m, \text{ where } v \text{ is the electron velocity}$$

The computed cyclotron radius is roughly commensurate with the above assumption, that the solenoid radius is 10  $\mu m$ .

## 9.2 Polarization of the Electron Gas Around the Nuclei

Simplification (7) models the nuclear charges as a uniform jellium, rather than charged points in space. The resulting electron orbitals are therefore not forming density cusps around the nuclei as one would expect to occur in reality.

It is intuitively clear, that the resulting binding energy with the jellium approach is higher (i.e. more endothermic) than in reality, where the electrons in the cusps on average come closer to the positive charge of the nuclei.

As an extension of the cylindrical model one can quantify the static electron polarization around the nuclei (i.e. cusps) by means of Thomas-Fermi screening. The contribution of the cusps to the total binding energy of a CP can be estimated with this.

Assuming the electron temperature in a CP is  $T_e < 10^5 K$  and the Fermi energy of the electrons (i.e. the difference between the highest and the lowest occupied electron eigenvalue) is  $\bar{E}_F > 10^5 eV$ , then  $k_B T_e < 8.6 eV \ll \bar{E}_F$ .

Therefore, Thomas-Fermi can be applied to a CP safely at the  $T_e \rightarrow 0$  limit.

For a Fermi gas at  $T = 0$  the state density at the Fermi edge is:

$$(190) \quad \frac{\partial n}{\partial \mu} = \frac{3}{2} \frac{n}{\bar{E}_F}, \text{ where } n \text{ is the electron number density and } \mu \text{ is the internal chemical potential}$$

Usually, the above equation is used for computing the screening wave number of Thomas-Fermi screening. However, the electron gas of a CP is not free, because it is bound to a potential well in radial direction.

As can be seen in Figure 17, the electron state density distribution in a CP differs from a free electron gas. The figure shows the state density distribution of a typical CP configuration. The maximum state density per electron is 11.6 MeV<sup>-1</sup>. The mean expectation value of the electron number density in this case is  $\langle n \rangle_{mean} = 0.150 pm^{-3}$ . The mean volume occupied by exactly one electron is  $V_{1e} = \langle n \rangle_{mean}^{-1} = 6.67 pm^3$ .

With these values the maximum state density per  $V_{1e}$  (i.e. the state density per volume at the Fermi edge) computes as:

$$(191) \quad \max \left( \frac{\partial n}{\partial \mu} \right) = \frac{11.6 \langle n \rangle_{mean}}{MeV} = \frac{1.74}{MeV \cdot pm^3}$$

The Fermi energy in this case is 157 keV. With this, equation (191) can be related to the Fermi energy like

With these values the maximum state density computes as:

$$(192) \quad \max \left( \frac{\partial n}{\partial \mu} \right) = \frac{11.6 \langle n \rangle_{mean}}{MeV} = 1.82 \frac{\langle n \rangle_{mean}}{\bar{E}_F}$$

For computing the Thomas-Fermi screening length in the region of highest electron density, equation (192) will be used below, rather than equation (190).

However, there are uncertainties, which could hamper the application of Thomas-Fermi screening to CPs:

- A strong magnetic field is present, with unclear (at least to the author) consequences to the polarization of the electrons
- It may be incorrect to assume full 3-D screening, because CPs mostly extend in axial direction and have a small radius (in the order of 40 pm, depending on configuration)

Additionally, the Fermi wave number  $k_F$  is not a well-defined quantity in CPs, because:

- The axial wave numbers at the occupation edge (Fermi level) are covering the hole range of k-values (in Figure 15), i.e. from  $55.6 \text{ pm}^{-1}$  through  $57.8 \text{ pm}^{-1}$ . The mean of these values is  $56.3 \text{ pm}^{-1}$ , which is translating into an axial De Broglie wave length of  $0.112 \text{ pm}$ .
- The axial wave numbers are greatly inflated/shifted by the magnetic field. Without this shift, the wave axial numbers at the Fermi level would probably be an order of magnitude smaller
- The maximum occupied wave number is greatly anisotropic in CPs. In radial direction the shortest De Broglie wave length is  $2.85 \text{ pm}$ , which translates to a wave number of  $2.20 \text{ pm}^{-1}$

The Thomas-Fermi model is valid only for wave numbers much smaller than the Fermi wave number  $k_F$ . In other words: Modeling the polarization cusps at distances to the nucleus shorter than  $2 \text{ pm}$  is probably of little value, because the Thomas-Fermi model is just not accurate in this range.

Despite all these uncertainties and in lack of a good alternative, the Thomas-Fermi theory will be applied in the following.

With linearized Thomas-Fermi screening the induced electron charge density is approximated by:

$$(193) \quad \bar{\sigma}_e^{\text{induced}}(\vec{r}_n) \approx -e^2 \max\left(\frac{\partial n}{\partial \mu}\right) \Phi^{\text{screened}}(\vec{r}_n) \approx -1.82e^2 \frac{\langle n \rangle_{\text{mean}}}{E_F} \Phi^{\text{screened}}(\vec{r}_n),$$

where  $\Phi^{\text{screened}}$  shall be the screened potential of a nucleus and  $\vec{r}_n$  is the position relative to the nucleus

In the above equation  $\Phi^{\text{screened}}$  is defined to approach zero at large  $\vec{r}_n$ .  $\langle n \rangle_{\text{mean}}$  is the value of the electron number density at large  $\vec{r}_n$ .

Relation (193) can be converted into a wave-number-dependent dielectric function (i.e. the relative permittivity):

$$(194) \quad \varepsilon_r(k) = 1 + \frac{k_s^2}{k^2}, \text{ where } k \text{ is the wave number of the polarization (in momentum space)}$$

$$\text{and } k_s = \sqrt{\frac{e^2}{\varepsilon_0} \max\left(\frac{\partial n}{\partial \mu}\right)} = \sqrt{\frac{1.82e^2}{\varepsilon_0} \frac{\langle n \rangle_{\text{mean}}}{E_F}} \text{ (in SI units) is the Thomas-Fermi screening wave number}$$

The dielectric function can be used to compute the effects of polarization in momentum space:

$$(195) \quad \varepsilon_r(k) = \frac{\bar{\sigma}^{\text{extern}}(k)}{\bar{\sigma}^{\text{extern}} + \bar{\sigma}_e^{\text{induced}}(k)} = 1 - \frac{\bar{\sigma}_e^{\text{induced}}(k)}{\bar{\sigma}^{\text{extern}} + \bar{\sigma}_e^{\text{induced}}(k)} = \frac{\Phi^{\text{extern}}(k)}{\Phi^{\text{extern}}(k) + \Phi_e^{\text{induced}}(k)}, \text{ where}$$

$\bar{\sigma}_e^{\text{induced}}(k)$  and  $\Phi^{\text{induced}}(k)$  are the electron charge density and the potential caused by polarization.  
 $\bar{\sigma}^{\text{extern}}(k)$  and  $\Phi^{\text{extern}}(k)$  are the charge density and the potential, which caused the polarization.

The Poisson's equation relates the electric potential with the volume charge density:

$$(196) \quad \nabla^2 \Phi(\vec{r}) = -\frac{\bar{\sigma}(\vec{r})}{\varepsilon_0}, \text{ where } \vec{r} \text{ is the position}$$

A nucleus with a point charge of  $Q_n = eZ$  will produce a Thomas-Fermi-screened potential of:

$$(197) \quad \Phi^{\text{screened}}(k) = \frac{e}{\varepsilon_0} \frac{Z}{k^2 + k_s^2}$$

The above equation Fourier-transforms to:

$$(198) \quad \Phi^{\text{screened}}(\vec{r}_n) = \frac{e}{4\pi\varepsilon_0} \frac{Z}{r_n} \exp(-k_s r_n), \text{ where } \vec{r}_n \text{ is the position relative to the nucleus}$$

The quantity  $1/k_s$  is the Thomas-Fermi screening length. With the values of  $\bar{E}_F = 157 \text{keV}$  and  $\langle n \rangle_{\text{mean}} = 0.150 \cdot \text{pm}^{-3}$  the screening length computes as:

$$(199) \quad \frac{1}{k_s} = \sqrt{\frac{\epsilon_0}{1.82e^2} \frac{\bar{E}_F}{\langle n \rangle_{\text{mean}}}} = 5.64 \text{ pm}$$

The screening length is a bit shorter than the minimum distance between the nuclei (7.66 pm for the same configuration). This might help to understand, why in a CP the nuclei can have such a high density.

Using (198) with (199), the screened potential is plotting as following:

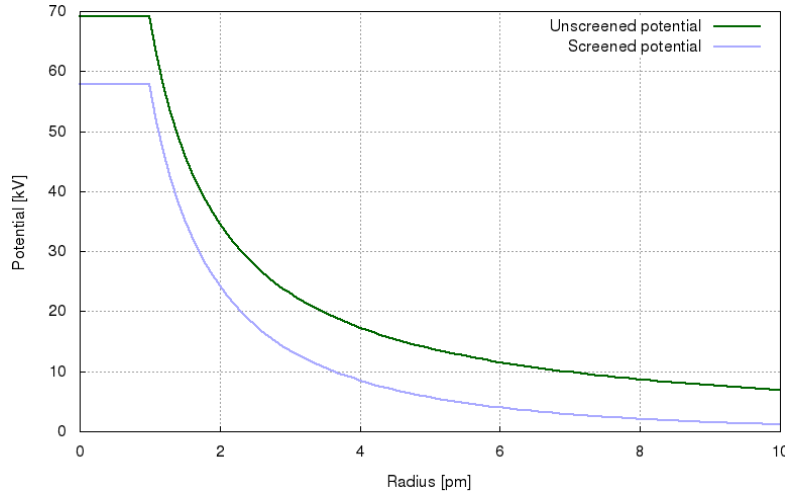


**Figure 8** Screened and unscreened potential of a nucleus with nuclear charge  $Z=48$ .  
The diverging values have been cropped at Radius  $< 1$  pm

The difference between the unscreened potential and the screened potential is not varying much with the radius. This difference can hence be characterized by a constant, i.e. the screening potential:

$$(200) \quad \Phi_s = \frac{eZk_s}{4\pi\epsilon_0} = 12.3 \text{ kV}, \text{ with } Z = 48 \text{ and } k_s^{-1} = 5.64 \text{ pm}$$

In line with the above example, for the fusion of hydrogen ( $Z=1$ ) with cadmium ( $Z=48$ ) the screening potential energy would be  $U_s = 12.3 \text{keV}$ . For d-d fusion there would be  $U_s = 256 \text{eV}$  and the minimum distance between neighboring deuterons would be 2.04 pm.

The induced electron density according to equation (193) is plotting as following:

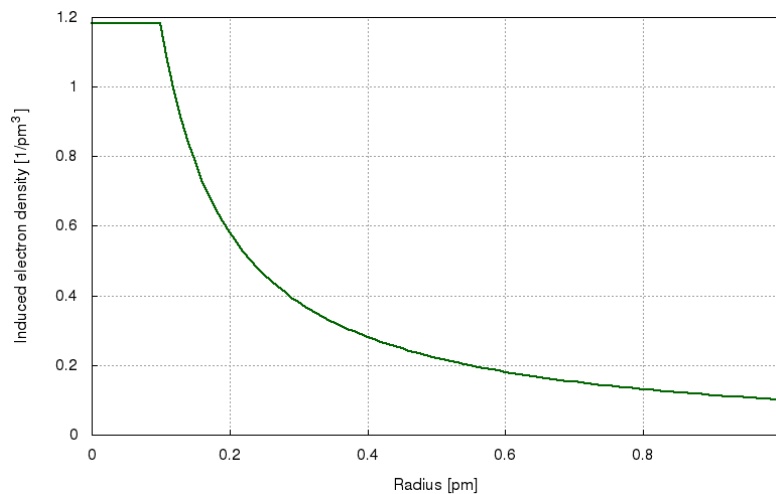


**Figure 9** Induced electron density around the nucleus of Figure 8.  
The diverging values have been cropped at Radius  $< 0.1$  pm

How much induced charge will be accumulated in a sphere around a nucleus (cusp) with a radius of one third of the distance to the nearest neighbor nucleus (2.47 pm)? This question can be answered by integrating equation (193) and using (198):

$$\begin{aligned}
(201) \quad Q_e^{cusp} &\approx -1.82e^2 \cdot 4\pi \frac{\langle n \rangle_{mean}}{\bar{E}_F} \int_0^{2.47 pm} \Phi^{screened}(\vec{r}_n) r_n^2 dr_n \\
&= -1.82 \frac{e^3 Z}{\epsilon_0} \frac{\langle n \rangle_{mean}}{\bar{E}_F} \int_0^{2.47 pm} r_n \exp(-k_s r_n) dr_n \\
&= 1.82 \frac{e^3 Z}{\epsilon_0} \frac{\langle n \rangle_{mean}}{\bar{E}_F k_s} \left[ r_n \exp(-k_s r_n) + \frac{1}{k_s} \exp(-k_s r_n) \right]_0^{2.47 pm} = -3.46e
\end{aligned}$$

The electron density  $\bar{\sigma}_e^{induced}/e$  surpasses  $\langle n \rangle_{mean} = 0.150/pm^3$  (i.e. the electron density at large  $\vec{r}_n$ ) only at  $r_n < 0.71 pm$ . For the purpose of estimating the binding energy contribution of the cusp, the integral can therefore be limited to maybe  $r_n < 0.71 pm$ .

The binding energy between a nucleus ( $Z=48$ ) and the charge induced by this nucleus in the cusp is:

$$\begin{aligned}
(202) \quad U_{cusp} &= 4\pi \int_0^{0.71 pm} \bar{\sigma}_e^{induced}(\vec{r}_n) \Phi^{unscreened}(\vec{r}_n) r_n^2 dr_n \\
&= -4\pi \cdot 1.82e^2 \frac{\langle n \rangle_{mean}}{\bar{E}_F} \int_0^{0.71 pm} \Phi^{screened}(\vec{r}_n) \Phi^{unscreened}(\vec{r}_n) r_n^2 dr_n \\
&= -\frac{1.82e^4 Z^2}{4\pi\epsilon_0^2} \frac{\langle n \rangle_{mean}}{\bar{E}_F} \int_0^{0.71 pm} \exp(-k_s r_n) dr_n \\
&= \frac{1.82e^4 Z^2}{4\pi\epsilon_0^2} \frac{\langle n \rangle_{mean}}{\bar{E}_F} \frac{1}{k_s} [\exp(-k_s r_n)]_0^{0.71 pm} = -69.6 keV
\end{aligned}$$

Dividing the result of equation (202) by the number of core electrons per nucleus (=48.96) yields an **estimated contribution of the cusp to the binding energy per electron of -1.42 keV**.

Given, that the contribution of the cusps is so small and there are so many uncertainties in applying Thomas-Fermi screening to CPs, the author decided to not include the cusp contribution in the Hamiltonian during the simulation runs.

### 9.3 Exchange-Correlation Energy Functionals

**Local-density approximations** (LDA) are approximations to the exchange-correlation energy functional in density functional theory (DFT) that depend solely upon the value of the electronic density at each point in space (and not, for example, derivatives of the density).

Using LDA for a CP (in units of the Hartree energy, cylindrical coordinates) provides:

$$(203) \quad E_{xc}[\sigma_e] = \frac{2\pi L}{\lambda_n} \int_0^\infty |\sigma_e(r)| \mathcal{E}_{xc}[\sigma_e] r dr,$$

where  $\sigma_e$  is the electron charge density in natural units according to (123),  $L$  is the axial length of the CP in units of the Bohr radius,  $r$  is the relative radius coordinate according to (122) and  $\mathcal{E}_{xc}$  is the exchange-correlation energy per particle of a homogeneous electron gas of charge density  $\sigma_e$ .

The exchange-correlation energy is decomposed into exchange and correlation terms linearly,

$$(204) \quad \mathcal{E}_{xc} = \mathcal{E}_x + \mathcal{E}_c$$

However, the DFT formalism breaks down, to various degrees, in the presence of a magnetic field. In such a situation, the one-to-one mapping between the ground-state electron density and wave function is lost. Generalizations to include

the effects of magnetic fields have led to the current density functional theory and magnetic field density functional theory. For reasons of simplicity, these theories are not engaged here.

The approximation quality of DFT/LDA achievable by neglecting the magnetic field is therefore seen as merely “experimental”. Nonetheless, such rogue approach is detailed below.

The analytically known exchange energy functional in LDA is (in units of the Hartree energy, cylindrical coordinates):

$$(205) \quad \varepsilon_x[\sigma_e] = -\frac{3}{4} \sqrt[3]{\frac{3}{\pi}} |\sigma_e(r)|$$

The Chachiyo correlation energy functional (in units of the Hartree energy), which is based on many-body perturbation theory, is applicable to the full range of densities:

$$(206) \quad \varepsilon_c[\sigma_e] = \frac{\ln(2)-1}{2\pi^2} \ln\left(1 + \frac{b}{r_s} + \frac{b}{r_s^2}\right),$$

$$\text{where } r_s = \sqrt[3]{\frac{3}{4\pi} \frac{1}{|\sigma_e|}} \text{ is the Wigner-Seitz parameter and } b = 20.4562557$$

The Wigner-Seitz parameter  $r_s$  is defined as the radius of a sphere which encompasses exactly one electron, divided by the Bohr radius.

With the CP configuration of chapter 10.1 the exchange energy per electron is -554 eV and the correlation energy per electron is -4.5 eV. These values are so small (compared to the other terms of the Hamiltonian), that they were not included in the simulation runs. Also, the values could be incorrect due to the strong magnetic field.